Continuous-variable quantum optical experiments in the time domain using squeezed states and heralded non-Gaussian states

Jun-ichi Yoshikawa*[a,b], Yosuke Hashimoto[a], Hisashi Ogawa[a], Shota Yokoyama[c], Yu Shiozawa[a], Takahiro Serikawa[a], Akira Furusawa[a]

[a]Department of Applied Physics, School of Engineering, The University of Tokyo, 7-3-1 Hongo, Bunkyo-ku, Tokyo 113-8656, Japan; [b]Quantum-Phase Electronics Center, School of Engineering, The University of Tokyo, 7-3-1 Hongo, Bunkyo-ku, Tokyo 113-8656, Japan; [c]Centre for Quantum Computation and Communication Technology, School of Engineering and Information Technology, University of New South Wales, Canberra, Australian Capital Territory 2600, Australia

ABSTRACT

Continuous-variable quantum information processing with optical field quadrature amplitudes is advantageous in deterministic creation of Gaussian entanglement. On the other hand, non-Gaussian state preparation and operation are currently limited, but heralding schemes potentially overcome this difficulty. Here, we summarize our recent progress in continuous-variable quantum optical experiments. In particular, we have recently succeeded in creation of ultra-large-scale cluster-type entanglement with full inseparability, multiplexed in the time domain; storage and on-demand release of heralded single-photon states, which is applied to synchronization of two heralded single-photon states; real-time quadrature measurements regarding non-Gaussian single-photon states with exponentially rising wavepackets; squeezing with relatively broader bandwidth by using triangle optical parametric oscillator.

Keywords: quantum optics, continuous variables, quantum entanglement, squeezed states, single-photon states, optical homodyne detection, optical parametric oscillator

1. INTRODUCTION

Quantum states of a light field can be represented either in the photon number basis, eigenstates of $\hat{n} = \hat{a}^\dagger \hat{a}$, or in the continuous quadrature amplitude basis, eigenstates of $\hat{x}$ or $\hat{p}$. They are related by $\hat{a} = (\hat{x} + i\hat{p})/\sqrt{2}$, and the commutation relation of continuous variables (CVs) $[\hat{x}, \hat{p}] = i$ is analogous to that of position and momentum operators. Reflecting these two bases, one is discrete and one is continuous, quantum optical experiments dealing with quantum information in a light field are typically classified into two types. One deals with photonic qubits $|\psi\rangle = \alpha|1,0\rangle + \beta|0,1\rangle$ (or more generally qudits) using photon detectors (counters), and the other deals with qumodes $|\psi\rangle = \int \psi(x)|x\rangle dx$ using homodyne detectors. However, since the Hilbert space of infinite-dimensional CV qumodes contains the Hilbert space of finite-dimensional qubits, continuous-variable quantum information processing may deal with encoded qubits. Famous examples are the Gottesman-Kitaev-Preskill qubits [1] and the coherent-state superposition (CSS) qubits [2]. Although such advanced hybrid quantum information processing is not yet achieved, there are already notable experimental achievements of incorporating qubits in continuous-variable systems. CV quantum teleportation of photonic time-bin qubits is successfully demonstrated [3,4]. Besides, another interesting experiment is reciprocal squeezing operation on single photon states converting to CSS-like states [5].

A strong advantage of CVs in quantum optics is that quantum entanglement is deterministically created from deterministically prepared squeezed states. On the other hand, it has been pointed out that CV processing within the Gaussian world is simulable [6]. Genuine non-Gaussian states, which have negative regions in their Wigner functions,

*yoshikawa@ap.t.u-tokyo.ac.jp

Advances in Photonics of Quantum Computing, Memory, and Communication X, edited by Zameer Ul Hasan, Philip R. Hemmer, Hwang Lee, Alan L. Migdall, Proc. of SPIE Vol. 10118, 1011804
 · doi: 10.1117/12.2252206

have been created probabilistically with heralding schemes, utilizing conditioning by photon detection [7-9]. When employing heralding schemes, the quantum states are naturally localized in the time domain. A Broader bandwidth of squeezing is preferable for the time-domain processing, because it can increase the number of qumodes per unit time.

Based on the above background, here we summarize our recent experimental progress. First, taking the advantage of CV entanglement creation, we have succeeded in creating extremely large scale of quantum entanglement in the cluster type, multiplexed in the time domain [10,11]. Second, we have succeeded in storing and on-demand releasing of non-Gaussian single photon states inside a concatenated cavity system [12], and by using this system the heralded single photon states are synchronized [13]. Third, we have demonstrated real-time quadrature measurements of non-Gaussian single-photon states [14]. Fourth, we are recently utilizing triangle optical parametric oscillators (OPOs), with which broadband squeezing have been created and detected [15].

2. EXPERIMENTS

2.1 Creation of cluster states multiplexed in the time domain

It has been theoretically known that any Gaussian entangled state can be created by combining single-mode squeezed states by a network of beam splitters [16, 17]. However, conventional optical CV schemes, allocating individual qumodes of a multimode quantum state to different light beams, are currently not suited for creation of large-scale entanglement, because of a limited space, a limited laser power, etc. This problem can be solved by multiplexing many qumodes in a light beam, either in the time domain [10,11,18] or in the frequency domain [19-21]. Note that these two multiplexing schemes are potentially combined [22].

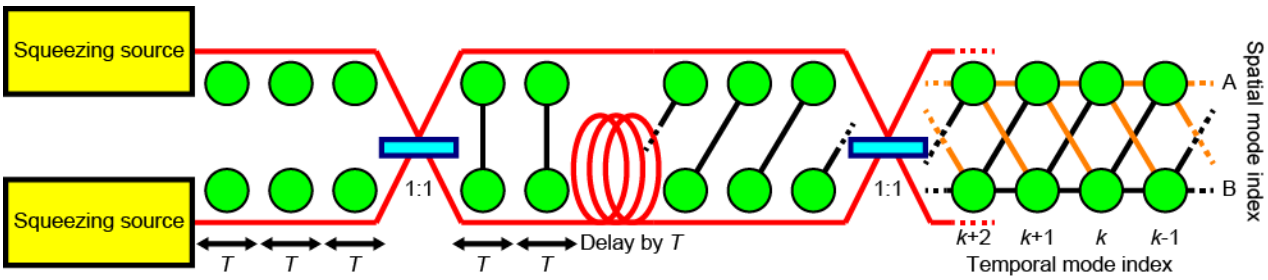

Figure 1. Schematic setup to create a dual-rail cluster state multiplexed in the time domain [10,11,18]. Two squeezing sources individually create a sequence of squeezed states, which is converted to a dual-rail cluster state by an asymmetric Mach-Zehnder interferometer. Each node represents a qumode, and each edge represents a correlation.

We are employing the time-domain multiplexing scheme. The schematic of creating a dual-rail cluster state multiplexed in the time domain is depicted in Fig. 1. The optical setup is two squeezed light sources followed by a Mach-Zehnder interferometer with asymmetric arms [10,11,18]. This setup in principle creates cluster states with an arbitrary number of modes in the longitudinal direction.

We demonstrated this scheme with two options, regarding the treatment of reference beams. In order to lock the optical system, we inject weak coherent modulated beams into individual squeezing sources as phase references. However, the modulated beams are noisy, and obscure the objective quantum correlations. Therefore, first, we chose the solution of blocking the reference beams for a short time when we verify the quantum correlation [10]. With this option, we have succeeded in creation of more than 10,000 modes with full inseparability. However, with this option, the optical system is not feedback controlled during the entanglement creation due to the absence of the reference beams, and thus uncontrolled drifts of the optical system gradually degrade the quantum correlations toward latter qumodes, which is the reason of the number of qumodes limited to around 16,000. To circumvent the degradation, we then tested the second option to continuously use the reference beams and instead to electrically filter out the noisy modulation frequencies from the homodyne signals before analog-to-digital conversion for data storage [11]. This choice sacrifices some freedom, as explained below. Each qumode composing the cluster state is not instantaneous but has a finite width in the time domain, and accordingly a quadrature value of each qumode is obtained by integrating the homodyne signal with some weight function. Unlike the first option where the weight functions well approximate the longitudinal optical modes, the electric

filters in the second option deform the modes. Consequently, the orthogonality between modes may be spoiled unless the weight functions are carefully selected. We selected weight functions that have both positive and negative parts, and succeeded in creation of cluster-type entanglement composed of more than one million qumodes with full inseparability [11].

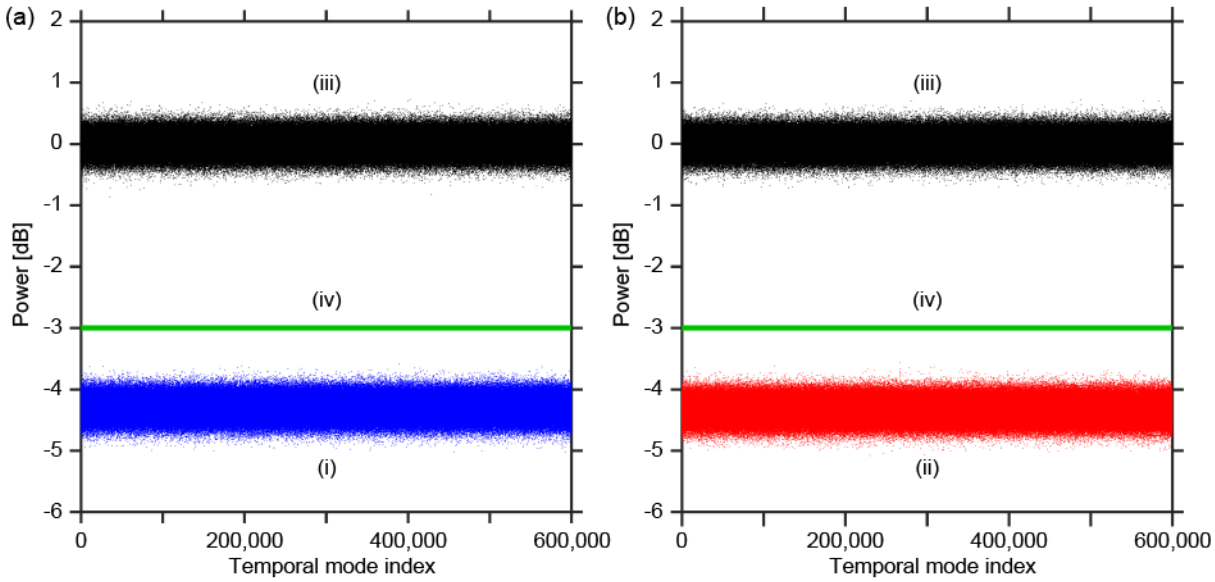

Figure 2. Quantum correlations for conjugate quadrature variables [11]. (i) Quantum correlations in x quadrature. (ii) Quantum correlations in p quadrature. (iii) Corresponding operators for reference vacuum states. (iv) Reference -3 dB line to represent a sufficient condition of full inseparability.

Figure 2 shows the experimental results obtained with the electric filtering option. A sufficient condition of full inseparability ($\hbar = 1$) is $\langle(\hat{x}_{A,k} + \hat{x}_{B,k} + \hat{x}_{A,k+1} - \hat{x}_{B,k+1})^2\rangle < 1$ and $\langle(\hat{p}_{A,k} + \hat{p}_{B,k} - \hat{p}_{A,k+1} + \hat{p}_{B,k+1})^2\rangle < 1$ for every temporal index k. This condition corresponds to squeezing more than -3 dB compared to the vacuum case. Taking into account the dual rail, the number of modes is about 1,200,000. We can see that the correlations never degrade toward latter, and that they are sufficiently squeezed, about -4.3 dB, in both of the conjugate quadratures, which is sufficient for full inseparability.

2.2 Storage and on-demand release of single photon states by means of cavities

Gaussian states are cheap in CV quantum optics, but they are not enough for quantum computation. Genuine non-Gaussian states are required to outperform classical computation [6]. Genuine non-Gaussian states, characterized by their negative Wigner functions, such as highly pure single-photon states, have been created by heralding schemes [7-9]. The heralding schemes utilize probabilistic projections by measurements onto non-Gaussian states, whose effects are transferred to the remaining light modes via quantum correlations. A simplest example is the creation of heralded single-photon states, where photon pairs are randomly generated by nonlinear optical effect and single-photon detection on the idler side projects the signal state onto a single-photon state. If the heralded single-photon state is sufficiently pure, its Wigner function has a region of negative values around the origin of the phase space, which can be checked by quantum homodyne tomography.

The heralding schemes are very powerful schemes enabling creation of various non-Gaussian states. However, a drawback is the randomness of its success. Therefore, quantum memories are important, which can preserve negativity of Wigner functions.

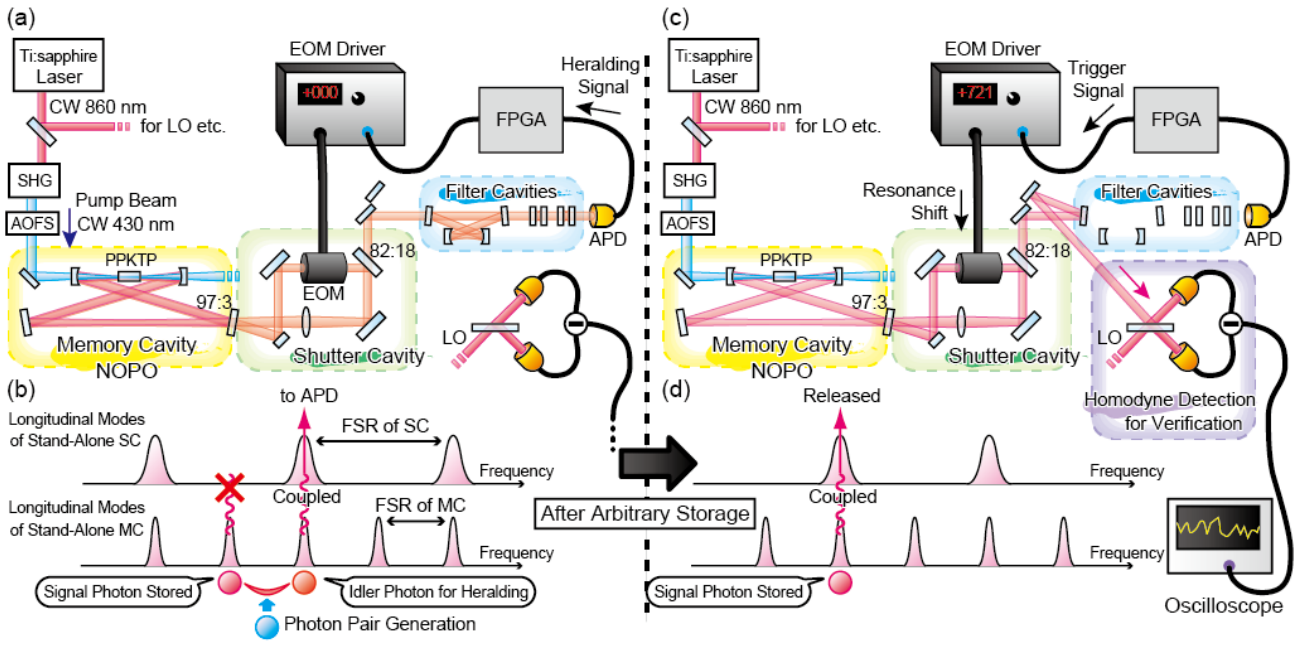

Figure 3. Schematic of memory storage of heralded single photon states based on concatenated cavities [12]. (a) Optical diagram in the storage phase. (b) Frequency diagram of the concatenated cavity system in the storage phase. (c) Optical diagram in the release phase. (d) Frequency diagram of the concatenated cavity system in the release phase.

We proposed all optical, cavity-based quantum memory for such storage, and experimentally demonstrated the storage for heralded single-photon states [12]. The schematic setup is shown in Fig. 3. At the output of the memory cavity, another cavity is concatenated, which works as a shutter. The shutter cavity contains an electro-optic modulator (EOM), which enables quick shift of the resonance frequency. The memory cavity contains a nonlinear optical crystal, and the photon pairs for the heralding scheme are created probabilistically inside the memory cavity. We choose the signal and idler to be frequency nondegenerate, separated by a free spectral range of the memory cavity. Initially, the shutter cavity is set to be resonant for the idler photon, while nonresonant for the signal photon. Therefore, when a photon pair is created inside the memory cavity, only the idler photon is emitted from the memory system, while the signal photon stays inside the memory cavity. The emitted idler photon is detected by a photon detector, yielding a herald signal. Once the single-photon state is stored inside the memory cavity, this state can be emitted from the memory system by shifting the resonance of the shutter cavity. In reality, the storage time is limited by internal losses of the memory cavity. This scheme can be in principle extended to other various heralded quantum states [8,9].

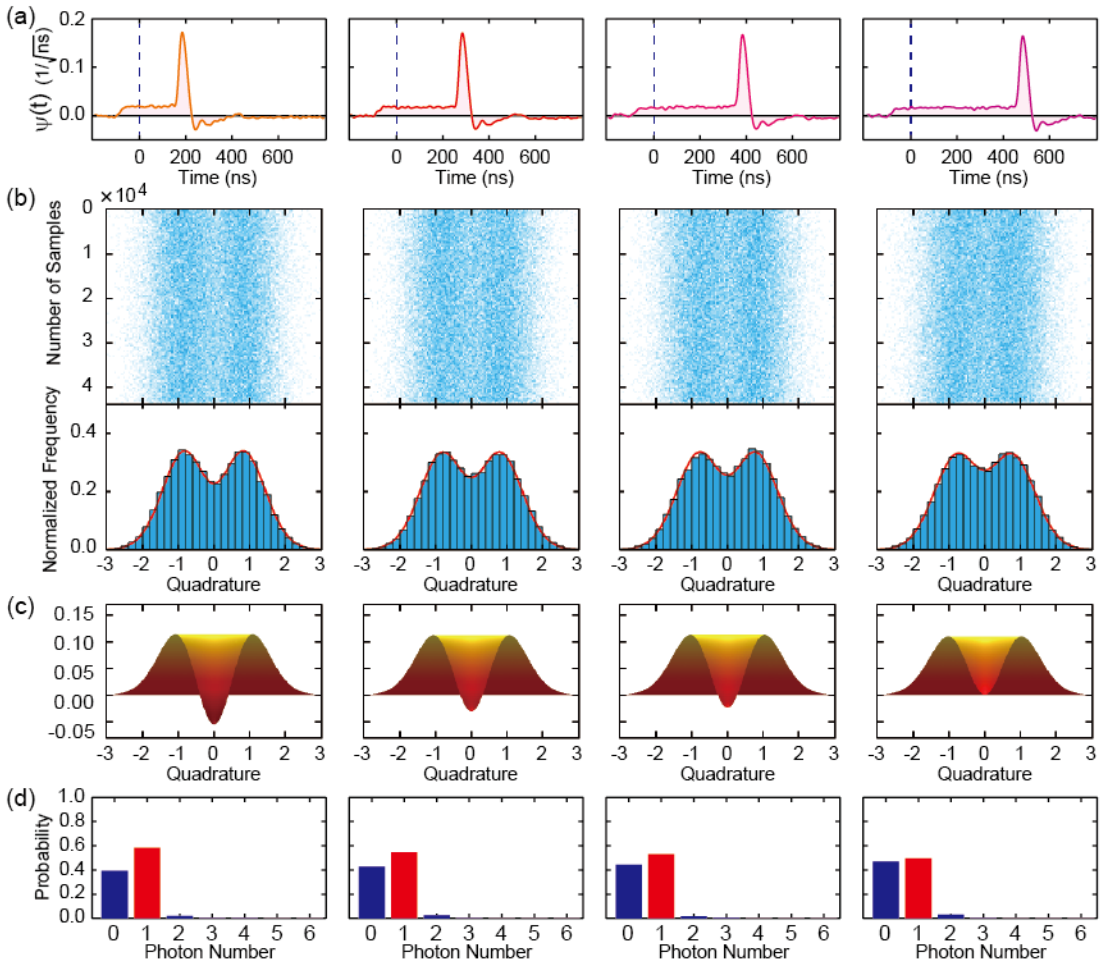

Figure 4. Experimental results of storing heralded single photon states [12]. The storage time is 0 ns, 100 ns, 200 ns, and 300 ns, from left to right, respectively. (a) Estimated temporal mode functions of the released single photon states. (b) Quadrature values. (c) Estimated Wigner functions. (d) Estimated photon number distributions.

The release timing relative to the heralding signal is controlled by a field-programmable gate array (FPGA), and the released single-photon states are characterized by homodyne detection. The experimental results of storing single-photon states are shown in Fig. 4 [12]. The four columns are, immediate release, release after 100 ns wait, 200 ns wait, and 300 ns wait, respectively, from left to right. The top panels are wavepacket of the single-photon state estimated from the homodyne signals. As expected, the peak of the wavepacket is correctly shifted step by step at intervals of 100 ns. Figure 4(b) shows the quadrature distribution corresponding to the wavepacket of Fig. 4(a). The distribution is highly non-Gaussian and there is a dip at the origin, which is the characteristic of single-photon states. Figure 4(c) is the Wigner function corresponding to the marginal distribution in Fig. 4(b), calculated on the assumption of rotational symmetry. The value at the origin is -0.054, -0.030, -0.024, and 0.001, from left to right, respectively. Figure 4(d) shows the photon number distribution equivalent to Fig. 4(c). The single photon fraction is 58.2%, 54.6%, 53.1%, and 49.7%, from left to right, respectively. Note that the single photon fraction over 50% is a sufficient condition of a negative Wigner function.

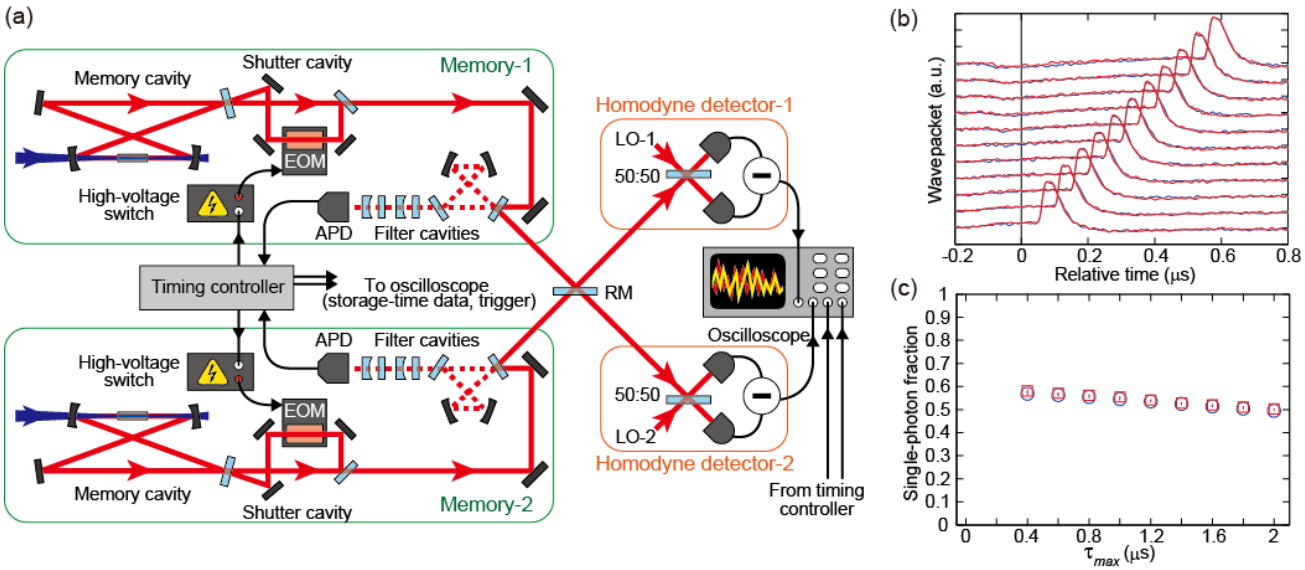

Figure 5. Photon synchronization experiment [13]. (a) Experimental setup. (b) Wavepackets released from individual memory systems, for various storage times. (c) Decay of average single-photon fractions from individual sources when the synchronization window $\tau_{\max}$ is widened.

By duplicating this concatenated cavity storage system, we also experimentally demonstrated synchronization of two heralded single photon states [13]. The setup is shown in Fig. 5(a). Since the pump beams are continuous wave, photon pairs are randomly created at any timing in both sides. However, even if the creation timing is somewhat different, synchronization is possible by keeping the earlier single-photon state unreleased until the other single-photon state is created and by releasing the two simultaneously. We first tested the individual photon memory systems. Fig. 5(b) shows the identicalness of the wavepackets of the released single photon states from the two memory systems, for various delay times. The wavepackets overlaps almost perfectly, and correctly shifted by the timing controller (FPGA). Then, by using them, we synchronized single photon states, varying the synchronization window. If the time difference between the two herald signals is within the window, the event is selected and released simultaneously. Figure 5(c) shows the decay of the single-photon fractions for individual memory systems when the synchronization window $\tau_{\max}$ is widened. The average single-photon fraction over 50% is kept for up to about 1800 ns of the synchronization window.

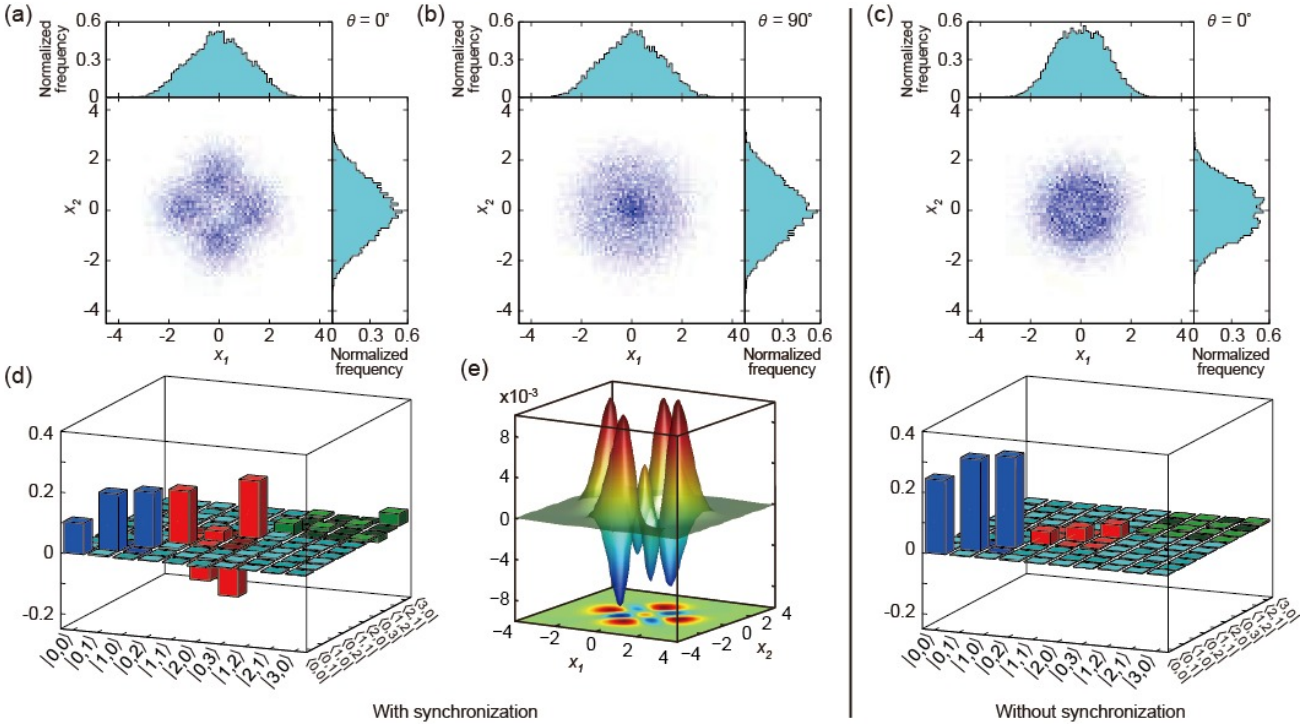

Figure 6. Hong-Ou-Mandel interference of synchronized single-photon states [13]. (a) Simultaneous quadrature distribution at some relative phase. (b) Simultaneous quadrature distribution at the relative phase shifted by 90 degrees from that of (a). (c) Simultaneous quadrature distribution without synchronization, where a single photon state comes from one input port and a vacuum state comes from the other input port. (d) Estimated density matrix calculated from simultaneous distributions including (a) and (b). (e) A cross section of the four-dimensional Wigner function which reflects the four-leaf clover structure of (a). (f) Estimated density matrix of the unsynchronized case (c).

The two synchronized single-photon states are used for the Hong-Ou-Mandel interference, and the output is characterized by two homodyne detectors. The resulting simultaneous distributions are shown in Fig. 6. Although the input single photon states are phase insensitive, the output two-mode state is entangled and has phase-sensitive correlation. Figure 6(a,b) are the two characteristic cases where the relative phases between the two local oscillators are different by 90 degrees. One is rotationally symmetric, while the other shows correlation like a four-leaf clover. Such phase sensitivity is not observed in the ordinary Hong-Ou-Mandel experiments testing only bunching of photons.

2.3 Real-time quadrature measurements on non-Gaussian continuous variables

We have seen that the heralding schemes can introduce non-Gaussian features in CV information processing. Then, the next desire is to use the non-Gaussian states in measurement-based information processing. In particular, we want to perform homodyne measurements on non-Gaussian CVs, which must be as quick as possible in order to utilize the measurement outcomes in later operations as feedforward. However, in this process, a bottleneck was integration of the homodyne signal with the weight determined by the longitudinal mode function of the target state. The longitudinal mode function of a heralded state is determined by optical filter effects of cavities. Conventionally, the integration has been performed by a computer after analog-to-digital conversion, which is far from real time. One thing to note is that feedforward of non-Gaussian CVs has already been utilized successfully in quantum teleportation [3,4,23]. This is because the feedforward in quantum teleportation is linear, in which case the integration can be postponed until the final stage of the output homodyne characterization. However, when we want to perform non-Gaussian quantum operations, the integration must be completed before the feedforward operations. This is the reason why we study real-time acquisition of integrated homodyne signals.

We demonstrated the real-time acquisition of non-Gaussian quadrature values of single-photon states, by creating the single-photon states in exponentially rising wavepackets [14]. In this case, a simple electric low-pass filter can perform the desired weighted integration continuously, and we obtain the desired quadrature values at known timings relative to the heralding signals.

The method of creating an exponentially rising mode of a single-photon state is to use a singly-resonant OPO with type-II phase matching crystal, pumped continuously. We insert a polarization beamsplitter inside the OPO, by which the signal light does not go around inside the cavity while the idler light is resonant and slowly goes out of the cavity. When an idler photon is detected as a herald, the heralded signal photon is always earlier, in a longitudinal mode inverse of the cavity exponential decay.

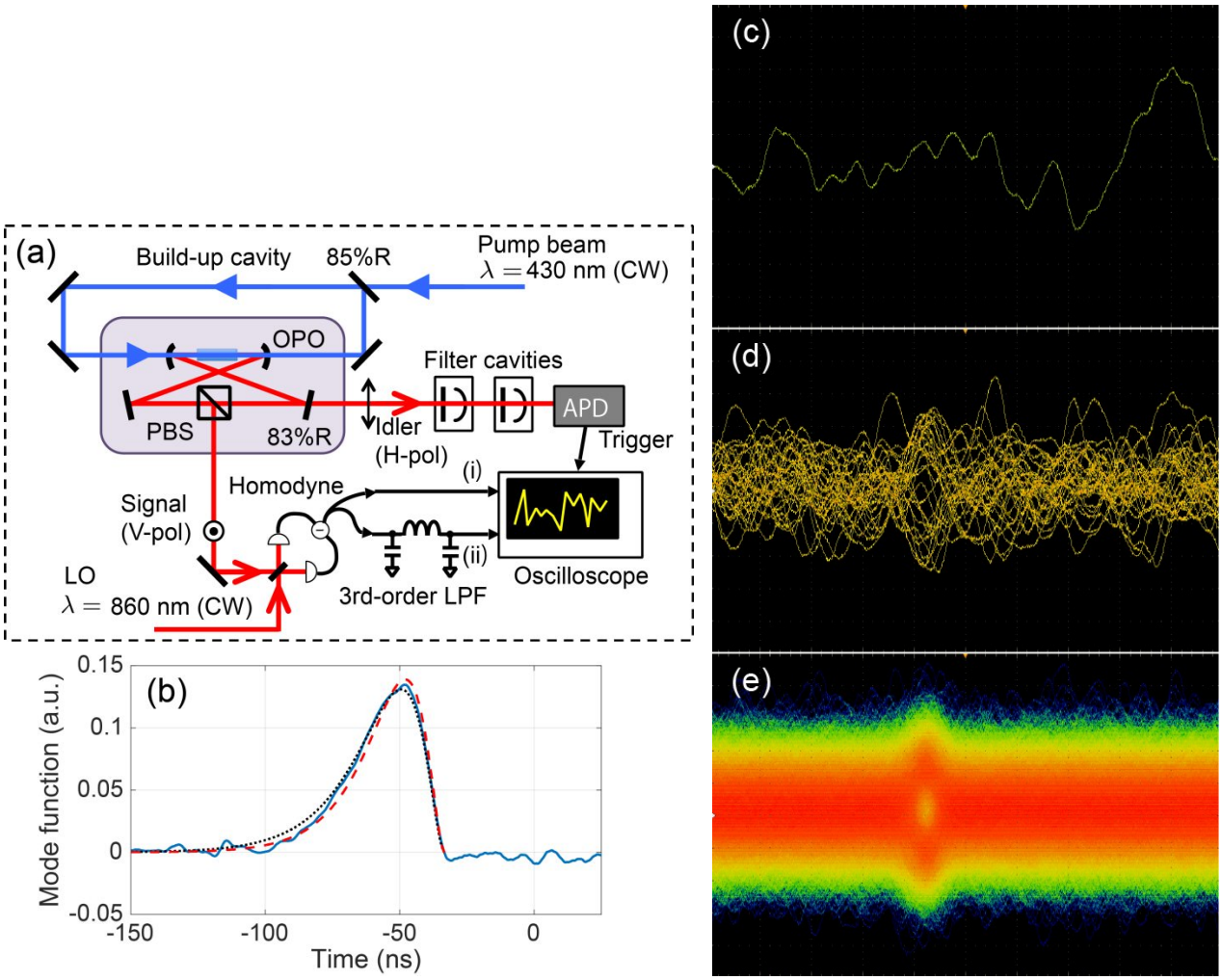

Figure 7. Real-time quadrature measurement of a single photon state [14]. (a) Experimental setup. (b) Exponentially rising mode. Solid blue: longitudinal mode function of single photon states estimated from the principal component analysis. Dashed red: effective weight function of the electric low-pass filter. Dotted black: longitudinal mode function expected from the bandwidths of the cavities. (c-e) Quadrature values obtained by continuous mode matching with the electric low-pass filter. Single trace, overlaid 32 traces, and overlaid 18,491 traces, respectively.

Figure 7 shows the experiment [14]. The homodyne signals after the electric low-pass filter are in Fig (c-e), where the effective weight function is continuously time-shifted. In Fig. 7(e), we can see at a timing a clear gap at the center of the distribution, which is the characteristic of the quadrature distribution of a pure single-photon state. Therefore, we have succeeded in obtaining single-photon quadrature values in real time as instant signals.

2.4 Squeezing with a small triangle optical parametric oscillator

As we have seen above, nonlinear optical effects are the key element of quantum optics, enabling creation of squeezed and entangled Gaussian states, and furthermore heralded non-Gaussian states. We are employing the OPO-based scheme, where nonlinear optical effects are enhanced by optical cavities. An advantage of the OPO-based enhancement compared with the waveguide-based enhancement is a clean output transverse mode in free space. It has been reported that the Fabry-Pérot type of OPOs can create high-level and broadband squeezed vacuum states [24,25]. However, we are interested in the other option, the ring type of OPOs. The advantage of a ring OPO is that clockwise and counterclockwise circulations are independent. This additional degree of freedom is used for control of the cavity and improves usability, which we think is important for application to large complicated systems. For the reasons above, we tested a small triangle OPO, and we succeeded in creation of high level and broadband squeezing [15].

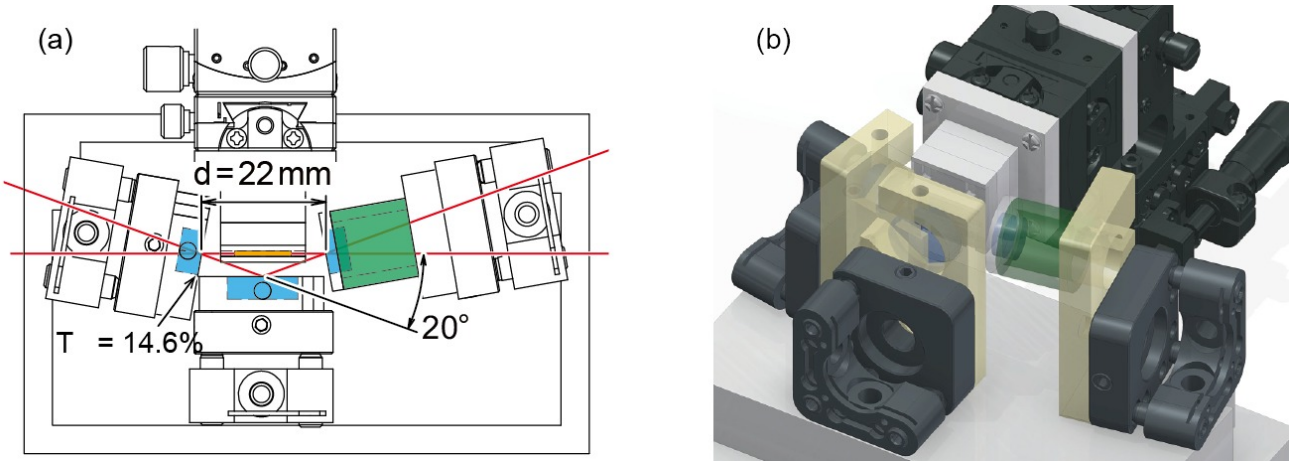

Figure 8. Design of a small triangle optical parametric oscillator [15]. (a) Top view. (b) Three-dimensional image.

The design of our triangle OPO is shown in Fig. 8 [15]. The nonlinear optical crystal is a periodically poled $KTiOPO_4$ crystal with a length of 10 mm, type-0 quasi-phase-matched at the wavelength of 860 nm. The crystal is placed between two curved mirrors, whose radius of curvature is 15 mm, and the third mirror is a flat mirror. The angle of incidence at the curved mirrors is 10 degrees. The transmissivity of the outcoupling mirror is 14.6%.

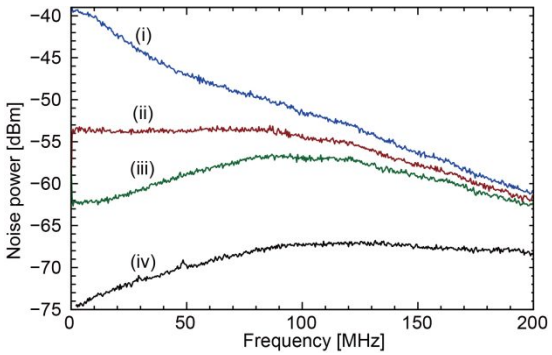

Figure 9. Homodyne spectra [15]. (i) Antisqueezed quadrature. (ii) Reference vacuum fluctuation. (iii) Squeezed quadrature. (iv) Electronic noise without the local oscillator.

The measured spectra of squeezed and anti-squeezed quadratures of the output squeezed vacuum, as well as the spectra of reference shot noise with the local oscillator of 18 mW and detector dark noise, are shown in Fig. 9 [15]. The power of the pump beam is about 225 mW. The half-width at half maximum linewidth of the OPO cavity is about 65 MHz, and the spectra are consistent with this bandwidth. The squeezing level at low frequency region is about -8.4 dB.

3. Conclusion

We have summarized our recent experimental achievements. We have succeeded in creation of ultra-large-scale cluster type of entanglement with full inseparability, with a scheme based on time-domain multiplexing [10,11]; storage and on-demand release of heralded single-photon states [12], and synchronization of two independent heralded single-photon sources [13]; real-time acquisition of a quadrature value of a non-Gaussian state in an exponentially rising wavepacket [14]; high-level and broadband squeezing by a small triangle OPO [15]. These technical achievements will be important for future development of CV quantum information processing, which potentially deals with encoded qubits.

Acknowledgments

This work was partly supported by PDIS and APSA commissioned by the MEXT, JSPS KAKENHI, CREST of the JST, and the SCOPE program of the MIC of Japan, and ARC CQC2T (Grant No. CE1101027) of Australia.

REFERENCES

[1] Gottesman, D., Kitaev, A. and Preskill, J., "Encoding a qubit in an oscillator," Phys. Rev. A 64, 012310 (2001).
[2] Ralph, T. C., Gilchrist, A., Milburn, G. J., Munro, W. J. and Glancy, S., "Quantum computation with optical coherent states," Phys. Rev. A 68, 042319 (2003).
[3] Takeda, S., Mizuta, T., Fuwa, M., van Loock, P. and Furusawa, A., "Deterministic quantum teleportation of photonic quantum bits by a hybrid technique," Nature 500, 315 (2013).
[4] Fuwa, M., Toba, S., Takeda, S., Marek, P., Mišta, L., Jr., Filip, R., van Loock, P., Yoshikawa, J. and Furusawa, A., "Noiseless conditional teleportation of a single photon," Phys. Rev. Lett. 113, 223602 (2014).
[5] Miwa, Y., Yoshikawa, J., Iwata, N., Endo, M., Marek, P., Filip, R., van Loock, P. and Furusawa, A., "Exploring a new regime for processing optical qubits: squeezing and unsqueezing single photons," Phys. Rev. Lett. 113, 013601 (2014).
[6] Mari, A. and Eisert, J., "Positive Wigner functions render classical simulation of quantum computation efficient," Phys. Rev. Lett.109, 230503 (2012).
[7] Lvovsky, A. I., Hansen, H., Aichele, T., Benson, O., Mlynek, J. and Schiller, S., "Quantum state reconstruction of the single-photon Fock state," Phys. Rev. Lett. 87, 050402 (2001).
[8] Bimbard, E., Jain, N., MacRae, A. and Lvovsky, A. I., "Quantum-optical state engineering up to the two-photon level," Nat. Photon. 4, 243 (2010).
[9] Yukawa, M., Miyata, K., Mizuta, T., Yonezawa, H., Marek, P., Filip, R. and Furusawa, A., "Generating superposition of up-to three photons for continuous variable quantum information processing," Opt. Express 21, 5529 (2013).
[10] Yokoyama, S., Ukai, R., Armstrong, S. C., Sornphiphatphong, C., Kaji, T., Suzuki, S., Yoshikawa, J., Yonezawa, H., Menicucci, N. C. and Furusawa, A., "Ultra-large-scale continuous-variable cluster states multiplexed in the time domain," Nat. Photon. 7, 982 (2013).
[11] Yoshikawa, J., Yokoyama, S., Kaji, T., Sornphiphatphong, C., Shiozawa, Y., Makino, K. and Furusawa, A., "Generation of one-million-mode continuous-variable cluster state by unlimited time-domain multiplexing," APL Photonics 1, 060801 (2016).
[12] Yoshikawa, J., Makino, K., Kurata, S., van Loock, P. and Furusawa, A., "Creation, storage, and on-demand release of optical quantum states with a negative Wigner function," Phys. Rev. X 3, 041028 (2013).
[13] Makino, K., Hashimoto, Y., Yoshikawa, J., Ohdan, H., Toyama, T., van Loock, P. and Furusawa, A., "Synchronization of optical photons for quantum information processing," Sci. Adv. 2, e1501772 (2016).
[14] Ogawa, H., Ohdan, H., Miyata, K., Taguchi, M., Makino, K., Yonezawa, H., Yoshikawa, J. and Furusawa, A., "Real-time quadrature measurement of a single-photon wave packet with continuous temporal-mode matching," Phys. Rev. Lett. 116, 223602 (2016).
[15] Serikawa, T., Yoshikawa, J., Makino, K. and Furusawa, A., "Creation and measurement of broadband squeezed vacuum from a ring optical parametric oscillator," Opt. Express 24, 28383 (2016).
[16] Braunstein, S. L., "Squeezing as an irreducible resource," Phys. Rev. A 71, 055801 (2005).
[17] van Loock, P., Weedbrook, C. and Gu, M., "Building Gaussian cluster states by linear optics," Phys. Rev. A 76, 032321 (2007).

[18] Menicucci, N. C., "Temporal-mode continuous-variable cluster states using linear optics," Phys. Rev. A 83, 062314 (2011).
[19] Menicucci, N. C., Flammia, S. T. and Pfister, O., "One-way quantum computing in the optical frequency comb," Phys. Rev. Lett. 101, 130501 (2008).
[20] Chen, M., Menicucci, N. C. and Pfister, O., "Experimental realization of multipartite entanglement of 60 modes of a quantum optical frequency comb," Phys. Rev. Lett. 112, 120505 (2014).
[21] Roslund, J., de Araújo, R. M., Jiang, S., Fabre, C. and Treps, N., "Wavelength-multiplexed quantum networks with ultrafast frequency combs," Nat. Photon. 8, 109 (2014).
[22] Alexander, R. N., Wang, P., Sridhar, N., Chen, M., Pfister, O. and Menicucci, N. C., "One-way quantum computing with arbitrarily large time-frequency continuous-variable cluster states from a single optical parametric oscillator," Phys. Rev. A 94, 032327 (2016).
[23] Lee, N., Benichi, H., Takeno, Y., Takeda, S., Webb, J., Huntington, E. and Furusawa, A., "Teleportation of nonclassical wave packets of light," Science 332, 330 (2011).
[24] Ast, S., Mehmet, M. and Schnabel, R., "High-bandwidth squeezed light at 1550 nm from a compact monolithic PPKTP cavity," Opt. Express 21, 13572 (2013).
[25] Vahlbruch, H., Mehmet, M., Danzmann, K. and Schnabel, R., "Detection of 15 dB squeezed states of light and their application for the absolute calibration of photoelectric quantum efficiency," Phys. Rev. Lett. 117, 110801 (2016).